

## **Investigation of Machining Parameters In EDM of Al-15%SiC<sub>p</sub> MMC Using Multichannel Electrode By ANOVA and ANN**

**S. Murugesan<sup>1\*</sup>, K. Balamurugan<sup>2</sup>, C. SathiyaNarayanan<sup>3</sup>**

<sup>1</sup>*Department of Mechanical Engineering, Government Polytechnic College, Trichy, Tamil Nadu, India- 620 022 e-mail: murugsslm6@gmail.com*

<sup>2</sup>*Department of Mechanical Engineering, Institute of Road and Transport Technology, Erode. Tamil Nadu, India-638 316.  
e-mail:drkbalamurugan@yahoo.co.in*

<sup>3</sup>*Department of Production Engineering, National Institute of Technology, Trichy. TamilNadu, India- 620015  
e-mail: csathiya@nitt.edu.*

### **Abstract**

The drilling of 6061Al-15% SiC<sub>p</sub> metal matrix composite (MMC) in die sinking electrical discharge machining (EDM) is analyzed, modeled and optimized in this research work. An electrolytic copper multichannel electrode is used as the tool. Three observed responses: material removal rates (MRR), electrode wear rate (EWR) and surface roughness (SR) are considered for this work. Electrode polarity (P), discharge current (I<sub>p</sub>), pulse on time (T<sub>on</sub>), pulse off time (T<sub>off</sub>) and dielectric pressure (P<sub>d</sub>) are considered as independent machining parameters. L<sub>18</sub> orthogonal array is used to conduct the experiments with various levels of P, I<sub>p</sub>, T<sub>on</sub>, T<sub>off</sub> and P<sub>d</sub>. The analysis of variance (ANOVA) reveals that T<sub>on</sub> is the most influential factor for MRR and SR, having highest degree of contribution of 46.37% .and 59.09% respectively. In case of EWR, current has the highest degree of contribution of 48.39% and is the most significant factor. A multilayer feed forward neural network is developed to model the machining process. The developed model is found to approximate the responses quite accurately. Moreover, the predicted results based on the above model have been confirmed with an unseen validation set of experiments and are found to be in good agreement with the experimental results. The proposed model can be employed successfully for the prediction of MRR, EWR and SR of the stochastic and complex EDM process. Based on this model, suitable machining conditions for achieving optimum values of MRR, EWR and SR are predicted and tested.

**Keywords:** Al-SiC MMC; EDM; ANN; ANOVA; Multichannel electrode

## Introduction

Aluminium metal matrix composites (AMMC) refer to the class of light-weight high-performance aluminium matrix material systems. The properties of AMMCs can be tailored to the demands of different industrial application by suitable combinations of matrix, reinforcement and processing route. The major advantages of AMMCs compared to unreinforced materials are greater strength, improved stiffness, reduced density, improved high temperature properties, controlled thermal expansion coefficient, enhanced electrical performance, improved abrasion, wear resistance and improved damping capabilities. Particle reinforced aluminium matrix composites (PAMC) constitute the largest quantity of composites produced and utilized on volume and weight basis. They are produced by PM/ stircast /melt infiltration/spraying /in situ processing techniques at industrial level. Particulates of SiC, Al<sub>2</sub>O<sub>3</sub>, TiC, TiB<sub>2</sub> and B<sub>4</sub>C have been used as reinforcements. PAMCs have been successfully used as components in automotive, aero-space, opto-mechanical assemblies and thermal management.

Machining aluminum metal matrix using EDM is one of the most extensively used non-conventional material removal processes. Its uniqueness, that is, the use of thermal energy to machine electrically conductive parts regardless of hardness has been its distinctive advantage.

K.H. Ho and S.T. Newman (2003) reported that the introduction of EDM to the metal cutting has been a viable machining option for producing highly complex parts, independent of the mechanical properties of the work piece material. Controlling the EDM process mostly relies on empirical methods largely due to the stochastic nature of the sparking phenomenon involving both electrical and non-electrical process parameters. The EDM process needs to be constantly revitalized to remain competitive in providing an essential and valuable role in the tool room manufacturing of part with difficult-to-machine materials and geometries.

Flushing conditions were improved by using rotary tube electrode by Mohan et al., (2004) in the study of effect of SiC and rotation of electrode on electric discharge machining of Al-SiC MMC. It was confirmed that EDM of blind hole drilling with a rotary tube electrode has a higher MRR, less electrode wear and better surface finish than solid stationary electrode. However, a mechanism required to rotate the tool was developed for this purpose. The electrode channel diameter and rotational speed had major effect on MRR, EWR and SR.

Artificial intelligence (AI) predictions have been gaining interest to a large extent in order to solve problems that are scarcely solved by the use of conventional methods. AI systems have the ability to be trained like humans, by accumulating knowledge through recurring learning activities.

Abeesh C. Basheer, et al (2008), created an ANN model for surface roughness in precision machining of metal matrix composites. In this model, a variation of the standard BP algorithm by using the Levenberg-Marquardt algorithm was used for training the system with 5-8-1 network configuration. Transigmoidal transfer function was used because of its symmetric nature. The predicted response of the ANN model was in very good agreement with the experimental data (correlation coefficient of 0.977 and the mean absolute error of 10.4%).

ANN was used to predict the surface roughness of metal matrix composites in addition to ANOVA by N. Muthukrishnan and J. Paulo Davim (2009). ANOVA and ANN approaches provide a systematic and effective methodology for optimization. A 3-layered multilayer perceptron using back propagation algorithm was used in the network with 3-10-1 configuration. This method was found to have prediction potentials for non-experimental patterns too. The ANN methodology consumed lesser time giving high accuracy with average error of 1.47%.

A hybrid model using ANN along with genetic algorithm was developed to model and optimize surface roughness in electrical discharge machining of Ti6Al4V, HE15, 15CDV6 and M-250 by G. Krishna MohanaRao et al (2009). A 4-4-1 network configuration was found to be the best structure for the model. Multilayer perceptron with hyperbolic tangent activation function was used to train the network. Good agreement between the neural predictions and experimental verification was demonstrated.

Mohan Kumar Pradhan and Chandan Kumar Biswas (2010) created Neuro-fuzzy and ANN models for prediction of MRR, TWR and radial overcut in die sinking EDM. Although both the models were found to be in good agreement with the experimental results, ANN was found to converge much faster.

The goal of the present study is to investigate the machining parameters for the formation of a blind hole of 12mm diameter and 5mm depth under the given machining conditions. The ANOVA is employed to explain the effect of the machining parameters on the characteristics of the EDM process. In addition ANN is used to model the stochastic EDM process and to predict the performance characteristics such as MRR, EWR and SR. This ANN model is then used to predict the output responses for various combinations all the possible input machining parameters. The optimum values of MRR, EWR and SR are found out from the set of predicted values. Confirmation experiments are conducted for these optimum machining parameter combinations and a comparison is made.

## **Experimental Details**

### **Equipment**

In order to obtain the data for modeling, a series of experiments were performed on a die-sinking electrical discharge machine SPARKONIX, which has servo controlled feed drive in the vertical direction. The electrical discharge machining conditions are given in Table1.

**Table 1:** Electrical discharge machining conditions

| Conditions                   | Description                          |
|------------------------------|--------------------------------------|
| Polarity of workpiece        | Positive and Negative                |
| Discharge current            | 4-12 A                               |
| Pulse on time                | 200-600 $\mu$ s                      |
| Pulse off time               | 20-60 $\mu$ s                        |
| Pressure of Dielectric fluid | 0.25-0.75 kg $\rho$ /cm <sup>2</sup> |
| Method of flushing           | Suction                              |

**Work Piece and Tool Material**

The workpiece used was 6061 Aluminium alloy reinforced with 15 % of SiC particles (by volume). The workpiece was a disc of 70 mm diameter and having 12 mm thickness. The specifications of the workpiece are given in Table 2.

**Table 2:** Work material specifications

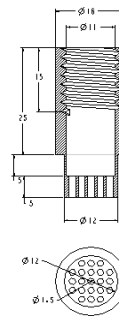
|                          |                              |
|--------------------------|------------------------------|
| Workpiece material       | 6061 Al-MMC                  |
| Al (%)                   | 92.7                         |
| Si (%)                   | 7.0                          |
| Mg (%)                   | 0.3                          |
| Reinforcement            | 15% SiC particles(by volume) |
| Particle size ( $\mu$ m) | 22                           |

The tool used was electrolytic copper multichannel electrode with an array of 21 channels, each of 1.5 mm diameter having 5mm depth as shown in Fig. 1.

Kerosene was used as the dielectric fluid and the suction flushing method was used for the effective flushing of machining debris from the working gap region.



a) Electrode



b) Sectional view

**Figure 1:** Multichannel electrode

**Experimental Procedure**

Prior to experimentation, the top and bottom surfaces of the workpiece were ground to make it flat and have a good quality surface finish. The bottom of the electrode was faced and polished by a fine grade emery sheet prior to every experimental run. Each experiment was run till a blind hole of 12mm diameter having 5mm depth was drilled. The machining time was measured with a stopwatch of accuracy 0.01s. The work piece as well as the tool were detached from the machine, cleaned and dried up, to make it free from the dielectric, dirt and debris. They were weighed, before and after machining, on a SHIMADZU precision electronic balance (maximum capacity 220 g, precision 0.001g). The surface roughness of the machined hole was measured using MITUTOYO SURFTEST surface roughness tester (range -200 to 150 microns, precision 0.02 microns). The average surface roughness  $R_a$  values were used to quantify the surface roughness. The cut-off length for each measurement was taken as 0.8mm. The raw and machined workpiece is shown in Fig.2. The SEM images of unmachined and machined surfaces are shown in Fig.3. The distribution of SiC particles in the Aluminium matrix is evident in Fig. 3a. The machined surface in Fig. 3b clearly shows the shear mode fracture along with pores.



a) Unmachined



b) Machined

**Figure 2:** Work piece

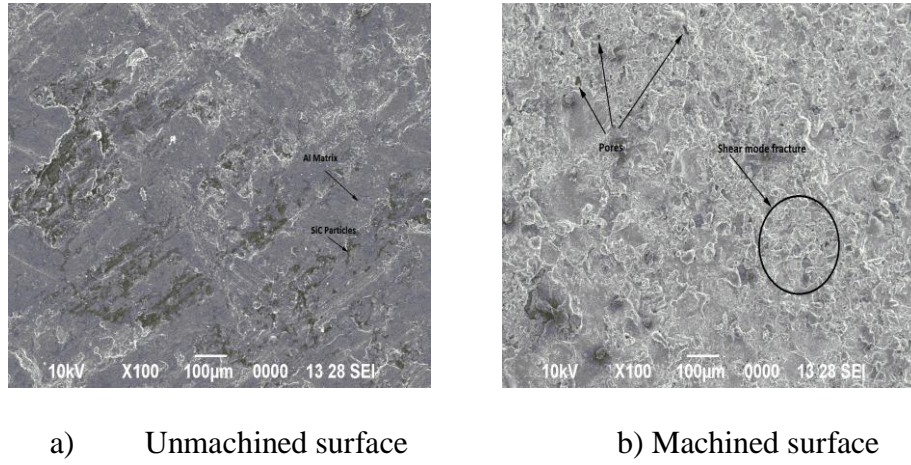


**Figure 3:** SEM images

### Machining Performance Evaluation

#### Material Removal Rate

MRR is calculated by using the weight loss ( $\Delta w_w$ ) from the workpiece and dividing it by the time of machining. In this attempt for blind hole drilling with multichannel electrode, two stages of machining were carried out. In the first stage of drilling, the rough machining was carried out using multichannel electrode resulting in fin like projections. These fins were removed manually using a chisel. In the second stage, a solid electrode was used to complete the blind drilling operation. Hence the total time of machining (T) is calculated as

$$T = T_1 + T_2 + T_3 \quad (1)$$

where,  $T_1$  : Time for machining with multichannel electrode

$T_2$  : Time for removing the fins

$T_3$  : Time for finishing with solid electrode.

Now,

$$MRR = \Delta w_w / T \quad (2)$$

#### Electrode Wear Rate

EWR is expressed as the weight loss of tool ( $\Delta w_t$ ) per unit time, expressed as

$$EWR = \Delta w_t / T \quad (3)$$

#### Surface Roughness

SR measured is the average surface roughness  $R_a$ . This is directly measured by using a surface roughness tester and is expressed in  $\mu\text{m}$ . Average of three readings is used as the measured values. The cut-off length is taken as 8mm.

### Experimental Design and Parameters Selection

The selected machining parameters, listed in Table 3, are polarity, discharge current, pulse on time, pulse off time and pressure of the dielectric fluid. The experiments

were planned according to Taguchi's L<sub>18</sub> (2<sup>1</sup>×3<sup>7</sup>) orthogonal array. Hence 18 experiments with one replication were conducted and their results are shown in Table 4. To eliminate the consequences of unaccounted factors of the responses, the experiments were carried out in random order. The outcome of this robust design facilitates to approximate all the main effects in this research.

Table 5 illustrates the analysis of variance (ANOVA) of MRR, EWR and SR: the columns of the table describing the degrees of freedom (DF), the F statistics and its percentage contribution. By comparing F statistic with tabulated values, it is concluded that the treatments have a statistically significant effect.

Keeping in view of the present research objectives, the experimental investigation and analysis were carried out for different parametric combinations, for deriving an effective representation of the model. As EDM process is stochastic and random in nature, it is very difficult to predict the output characteristics accurately by a mathematical equation. So an ANN has been implemented here to model the die sinking EDM process. This technique is especially worthwhile in processes where a dynamic nonlinear relationship exists and a complete understanding of the physical mechanisms is very difficult, as in the case of EDM process. One of the advantages of these approaches is that a model can be constructed very easily based on the given inputs and outputs and can be trained to predict the process responses.

**Table 3:** Machining parameters and their levels

| Machining parameter | Symbol | Level 1 | Level 2 | Level 3 |
|---------------------|--------|---------|---------|---------|
| Polarity            | A      | +       | -       |         |
| Discharge current   | B      | 4       | 8       | 12      |
| Pulse on time       | C      | 200     | 400     | 600     |
| Pulse off time      | D      | 20      | 40      | 60      |
| Dielectric pressure | E      | 0.25    | 0.5     | 0.75    |

**Table 4:** Experiment Results

| Trial No | Polarity | Current (amps) | Pulse on Time( $\mu$ s) | Pulse off Time( $\mu$ s) | Pressure kg/ cm <sup>2</sup> | MRR (mg/min) | EWR (mg/min) | SR ( $\mu$ m) |
|----------|----------|----------------|-------------------------|--------------------------|------------------------------|--------------|--------------|---------------|
| 1        | +        | 4              | 200                     | 20                       | 0.25                         | 23.58        | 5.28         | 3.88          |
| 2        | +        | 4              | 400                     | 40                       | 0.5                          | 44.90        | 3.19         | 5.93          |
| 3        | +        | 4              | 600                     | 60                       | 0.75                         | 50.56        | 1.89         | 5.30          |
| 4        | +        | 8              | 200                     | 20                       | 0.5                          | 24.27        | 14.89        | 4.26          |
| 5        | +        | 8              | 400                     | 40                       | 0.75                         | 104.69       | 14.33        | 6.06          |
| 6        | +        | 8              | 600                     | 60                       | 0.25                         | 118.94       | 6.11         | 8.41          |
| 7        | +        | 12             | 200                     | 40                       | 0.25                         | 43.93        | 13.06        | 5.61          |
| 8        | +        | 12             | 400                     | 60                       | 0.5                          | 109.47       | 9.74         | 7.31          |
| 9        | +        | 12             | 600                     | 20                       | 0.75                         | 196.84       | 9.20         | 9.72          |
| 10       | -        | 4              | 200                     | 60                       | 0.75                         | 18.45        | 7.22         | 3.92          |
| 11       | -        | 4              | 400                     | 20                       | 0.25                         | 83.62        | 4.59         | 5.23          |
| 12       | -        | 4              | 600                     | 40                       | 0.5                          | 93.63        | 3.76         | 8.51          |
| 13       | -        | 8              | 200                     | 40                       | 0.75                         | 43.84        | 28.68        | 5.39          |
| 14       | -        | 8              | 400                     | 60                       | 0.25                         | 108.77       | 22.77        | 7.15          |
| 15       | -        | 8              | 600                     | 20                       | 0.5                          | 183.95       | 12.22        | 8.86          |
| 16       | -        | 12             | 200                     | 60                       | 0.5                          | 50.99        | 33.45        | 5.83          |
| 17       | -        | 12             | 400                     | 20                       | 0.75                         | 203.30       | 29.99        | 7.79          |
| 18       | -        | 12             | 600                     | 40                       | 0.25                         | 294.78       | 19.62        | 12.20         |

**Table 5:** Analysis of variance for MRR, EWR and SR

| Source           | DF | MRR   |                | EWR   |                | SR    |                |
|------------------|----|-------|----------------|-------|----------------|-------|----------------|
|                  |    | F     | % Contribution | F     | % Contribution | F     | % Contribution |
| P                | 1  | 6.79  | 7.48%          | 15.14 | 24.29%         | 6.56  | 4.75%          |
| I                | 2  | 13.18 | 29.05%         | 17.13 | 48.39%         | 17.25 | 24.95%         |
| T <sub>on</sub>  | 2  | 21.03 | 46.37%         | 0.74  | 15.37%         | 40.84 | 59.09%         |
| T <sub>off</sub> | 2  | 2.65  | 5.83%          | 0.48  | 0.23%          | 2.45  | 3.54%          |
| Pd               | 2  | 1.11  | 2.44%          | 4.93  | 2.13%          | 1.30  | 1.88%          |
| Error            | 8  |       | 8.82%          |       | 9.58%          |       | 5.79%          |
| Total            | 17 |       | 100%           |       | 100%           |       | 100%           |

## ANN Model

An artificial neuron network (ANN) is a computational model based on the structure and functions of biological neural networks. Information that flows through the network affects the structure of the ANN because a neural network changes, or learns-in a sense, based on that input and output.

ANNs are considered nonlinear statistical data modeling tools where the complex relationships between inputs and outputs are modeled or patterns are found.

For this reason, the intention of this research is to propose a model using the ANN approach to predict the responses such as MRR, EWR and SR.

## ANN Architecture

A multilayer feed forward network with five input neurons, one hidden layer and one output neuron is used and the architecture of this model is depicted in Fig. 4. The



neural network model is developed using the Neural Tools package. The activation function in the hidden layer neurons is a hyperbolic tangent sigmoid transfer function. The output neuron uses identity as the activation function; that is, it simply returns the weighted sum of inputs. The training algorithm used in the Neural Tools package is “Conjugate Gradient Descent” method belonging to the category of “second order” optimization methods for faster training. The stochastic “Simulated Annealing” method is used along with the Conjugate Gradient Descent method to reduce the risk of finding the local rather than the global minimum. The algorithm decides which method to use at a particular point, based on the results of previous trials. The scale of the input and output data is an important matter to consider, especially when the operating ranges are different. This scaling or normalizing is done to equalize the effect of variables on the net output during the initial stages of training. Mapping each term to a value between -1 and 1 using linear mapping does the scaling.

$$N = [ (R-R_{min}) \times (N_{max}-N_{min}) / (R_{max}-R_{min}) ] + N_{min} \tag{4}$$

The data set obtained from the experiments is divided randomly into two subsets, namely training and testing. The training set is used to calculate the gradient and to form the weight factors and bias. The testing data is used to minimize the root square error (MSE) while training and to stop the training after appropriate trials. The verification experiment data set, shown in Table 6, is used to calculate the prediction error to estimate the accuracy of the model on the unseen data set.

**Input layer Hidden layer Output layer**

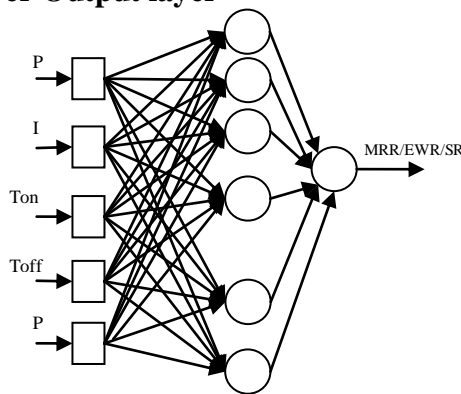
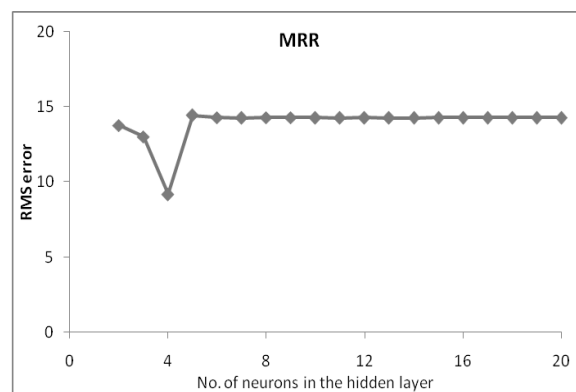


**Figure 4:** Neural Network Architecture

**Table 6:** Verification experiment

| Expt no | P | I <sub>p</sub> (amps) | T <sub>on</sub> (μs) | T <sub>off</sub> (μs) | P <sub>d</sub> (kg/cm <sup>2</sup> ) | MRR (mg/min) | EWR (mg/min) | SR (μm) |
|---------|---|-----------------------|----------------------|-----------------------|--------------------------------------|--------------|--------------|---------|
| 1       | + | 4                     | 200                  | 40                    | 0.75                                 | 26.52        | 6.12         | 4.10    |
| 2       | - | 4                     | 400                  | 60                    | 0.5                                  | 93.20        | 6.58         | 4.62    |
| 3       | + | 8                     | 200                  | 40                    | 0.75                                 | 28.66        | 15.62        | 4.18    |
| 4       | - | 8                     | 400                  | 20                    | 0.75                                 | 170.82       | 23.84        | 5.68    |
| 5       | + | 12                    | 400                  | 20                    | 0.25                                 | 176.94       | 10.38        | 8.90    |
| 6       | - | 12                    | 600                  | 60                    | 0.25                                 | 288.96       | 21.88        | 11.48   |

An ANN has one input layer and one output layer with one or more hidden layers in between, whose computational nodes are respectively called hidden neurons. The selection of the number of hidden neurons is a crucial decision, as it affects how well the network is able to process the data. The number of hidden neurons is established using a simple trial-error method in all applications on the basis of least root mean square error (RMS) in the testing data set. During the training, the RMS of the testing data is recorded after maximum trials and these are plotted against the number of nodes in the hidden layer for MRR, EWR and SR- as shown in Fig. 5. The plot illustrates that there is an optimal number of nodes where the RMS, for each of the responses, exhibit a minimum value. The number of nodes in the hidden layer is found to be 4, 5 and 4 for MRR, EWR and SR respectively. As there are five inputs and one output, the number of neurons in the input and output layer has to be set 5 and 1 respectively. Also for the majority of the applications, one hidden layer is selected for MLFN. Hence only one hidden layer is adopted. Therefore, 5-1-1 ANN architecture is considered for the modeling of the responses and trained. Now, the models are ready to predict the validation data set.



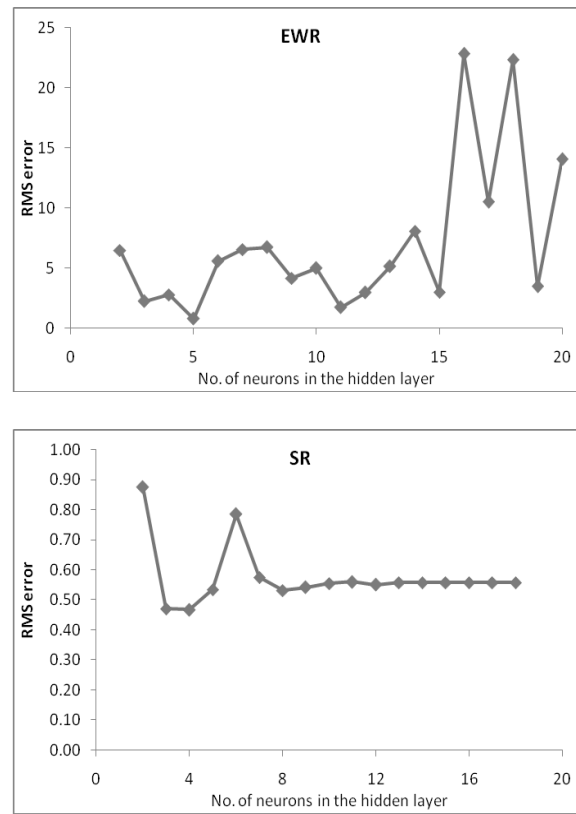


**Figure 5:** Optimal number of neurons in the hidden layer

## Results and Discussion

In this research, ANOVA has been carried out and an ANN model has been developed for MRR, EWR and SR in EDM process. Five machining parameters namely Electrode polarity (P), discharge current ( $I_p$ ), pulse on time ( $T_{on}$ ), pulse off time ( $T_{off}$ ), and dielectric pressure ( $P_d$ ) are considered as input parameters. Taguchi's  $L_{18}$  orthogonal array is used to develop the data for ANOVA and ANN. ANOVA results exhibit the impact of each input parameter in this EDM process. The predicted values from ANN model are compared with the actual experimental data in terms of residuals and the average prediction error for all the responses. From the ANN model, the values of MRR, EWR and SR are predicted for all the 162 combinations ( $2^1 \times 3^4 = 162$ ) of this experimental work. The optimum values for MRR, EWR and SR are obtained and verified experimentally.

## Analysis on Responses

The following discussion focuses mainly on the essential parameters which largely contribute to the Taguchi methodology. Herein, the blind hole drilling in EDM was verified by inspecting the MRR, EWR and SR.

### Effect on MRR

Fig. 6 presents the curves of MRR under various machining conditions. Fig. 6a depicts the MRR with positive and negative polarity of the machining conditions. According to this figure, the MRR was higher with a negative polarity (i.e., the workpiece as cathode and the electrode as anode) than with the positive polarity. This phenomenon might be attributable to the transfer of energy during the discharging process. The transfer of energy during charging process was more when the workpiece was kept at negative polarity than at positive.

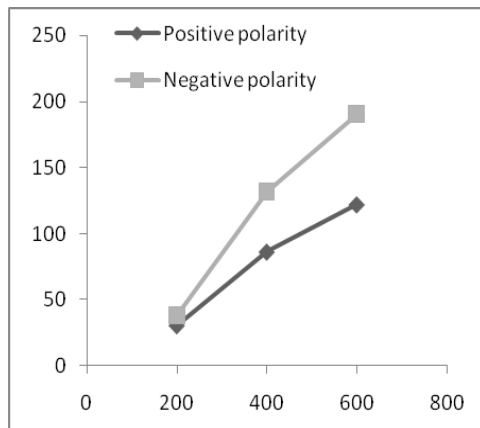


Fig. 6a

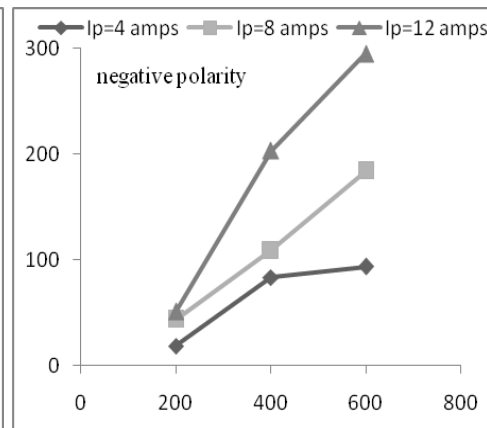


Fig. 6b

**Figure 6:** MRR versus EDM parameters

Fig. 6b presents the MRR versus pulse duration under various discharge currents. According to this figure, MRR increased with the discharge current. This is expected because an increase in pulse current produces strong spark, which produces higher temperature, causing more material to melt and erode from the work piece. It is expected that when  $T_{on}$  increases, the MRR usually increases up to a maximum value after which it starts to fall. The plot represents the values before the peak has reached.

### Electrode Wear Rate

Fig.7 shows the EWR under various machining conditions. Fig. 7a depicts EWR versus pulse duration under various discharge currents.

According to this figure, the EWR is either increased by discharge current or decreased by pulse duration. The discharging energy is consumed in the erosion of material, in the discharge channel and in the electrode. The discharging energy for EDM is defined as

$$W_e = \int_0^t E(t)I(t)dt \quad (5)$$

Where  $W_e$  denotes the discharge energy,  $E$  represents the discharge voltage,  $I$  is the peak current and  $t$  is the pulse duration.

Thus, a large peak current may generate a large discharging energy and cause a large EWR. The EWR increases in an inverse relation to pulse duration. The phenomenon may be attributable to the electrode being made of copper, which has a higher thermal conductivity than that of any other metal. Thus, the heat generated during the machining was easily removed, the rapid heat removal facilitating a reduction of the temperature around the surface of the copper electrode for longer pulse duration.

Fig. 7b depicts the EWR versus pulse duration under different polarities. According to this figure, the EWR was higher under a negative polarity than for a positive polarity. This phenomenon also corresponds to what the MRR implied for a transfer of energy, as mentioned earlier.

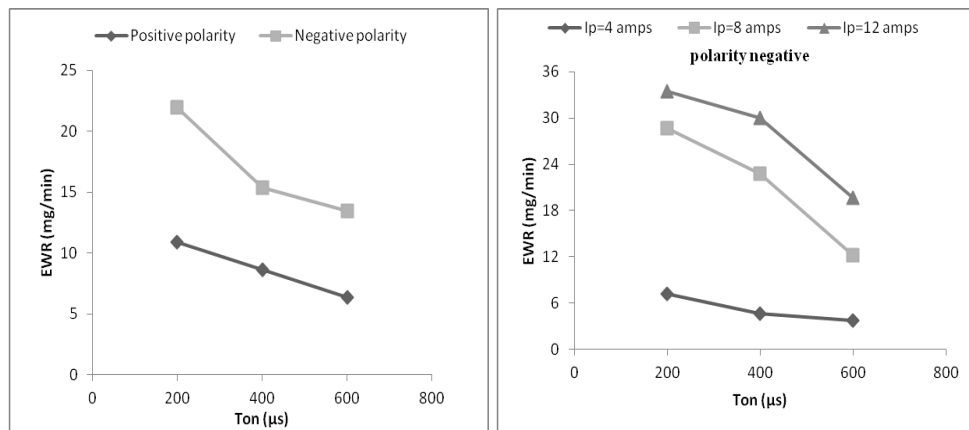


Fig. 7a Fig. 7b  
**Figure 7: EWR versus EDM parameters**

*Surface Roughness*

Fig. 8 evaluates the SR under various machining conditions. Fig. 8a depicts the SR versus pulse duration under various discharge currents. According to this figure, the SR increases with discharge current. This event might be due to generation of larger crater on the surface of the workpiece during larger discharging energy.

Fig. 8b shows the effect of polarity adopted in the EDM. With a negative polarity used in EDM process, the craters of the workpiece surface may have an irregular profile. With positive polarity, in contrast, the craters may be flatter.

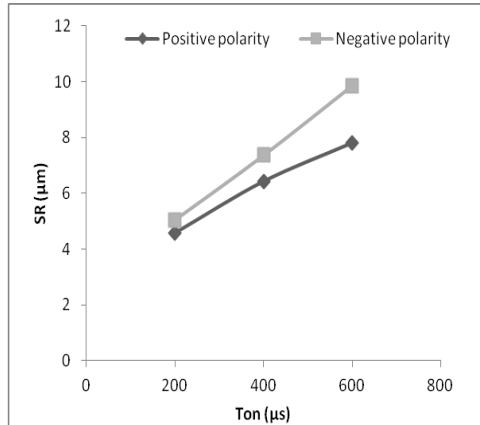


Fig. 8a

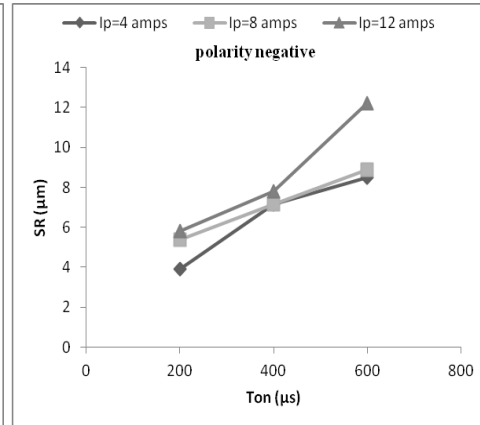


Fig. 8 b

**Figure 8:** SR versus EDM parameters

### Model Validation

The generalization capability of any model can be well judged only with a completely unused data set. Hence, it is decided to test all the models using totally unseen data, not previously used for training as well as testing purpose. If these developed models succeed the validation process, it connotes that the model can be useful not only to the parameter range of experimental conditions used in model building but also to the range of experimental conditions used in the model validation. Accordingly, an experimental approach is adopted, which involves testing the trained neural networks against another set of experimental data illustrated in Table 6 that are again drawn randomly. However, the set of combinations is different from one used in training the network. These experimentally obtained values are compared with the predicted values and the prediction error is obtained for each of the performance parameter. Prediction error has been defined as follows:

$$\text{Prediction error \%} = (|\text{Expt. Value} - \text{Pred. value}| / \text{Expt. Value}) * 100 \quad (6)$$

**Table 7:** Comparison of experimental results with the ANN model prediction

| Expt no                            | Experimental results |              |         | ANN model predictions |              |         | Prediction error (%) |       |       |
|------------------------------------|----------------------|--------------|---------|-----------------------|--------------|---------|----------------------|-------|-------|
|                                    | MRR (mg/min)         | EWR (mg/min) | SR (μm) | MRR (mg/min)          | EWR (mg/min) | SR (μm) | MRR                  | EWR   | SR    |
| 1                                  | 26.52                | 6.12         | 4.10    | 32.85                 | 7.65         | 4.29    | 23.87                | 25.00 | 4.63  |
| 2                                  | 93.20                | 6.58         | 4.62    | 103.76                | 7.57         | 5.01    | 11.33                | 15.05 | 8.44  |
| 3                                  | 28.66                | 15.62        | 4.18    | 33.21                 | 14.32        | 4.29    | 15.88                | 8.32  | 2.63  |
| 4                                  | 170.82               | 23.84        | 5.68    | 195.30                | 27.06        | 4.37    | 14.33                | 13.51 | 23.06 |
| 5                                  | 176.94               | 10.38        | 8.90    | 194.65                | 9.78         | 8.33    | 10.01                | 5.78  | 6.40  |
| 6                                  | 288.96               | 21.88        | 11.48   | 295.62                | 23.43        | 10.96   | 2.30                 | 7.08  | 4.53  |
| Average prediction error (%)       |                      |              |         |                       |              |         | 12.95                | 12.46 | 8.28  |
| Total average prediction error (%) |                      |              |         |                       |              |         | 11.23                |       |       |

Comparisons of predicted and experimental values are listed in Table 7 for MRR, EWR and SR. To estimate the precision of the prediction model, percentage

prediction error and average prediction error were used. The average prediction error is calculated by averaging the prediction error of responses. The experimental values were evaluated with the predicted values from the developed models, and it was found that the average prediction errors of MRR, EWR and SR are 12.95%, 12.46% and 8.28% respectively. Consequently the prediction accuracy of the model emerges to be agreeable.

**Optimization**

For the 162 possible combinations of this experimental work, the values of MRR, EWR and SR are predicted using this ANN model. The optimum values for MRR, EWR and SR are obtained from this ANN model. The input parameters for the optimum conditions are listed in Table 8. These optimum machining conditions are verified experimentally, compared with predicted values and shown in Table 9.

**Table 8:** Input parameters for optimum conditions

| Response | Polarity P | Current I <sub>p</sub><br>Amps | Pulse on Time<br>T <sub>on</sub> μs | Pulse off Time<br>T <sub>off</sub> μs | Pressure<br>Pd kg/ cm <sup>2</sup> |
|----------|------------|--------------------------------|-------------------------------------|---------------------------------------|------------------------------------|
| MRR      | -          | 12                             | 600                                 | 60                                    | 0.5                                |
| EWR      | +          | 4                              | 400                                 | 40                                    | 0.25                               |
| SR       | +          | 4                              | 200                                 | 60                                    | 0.5                                |

**Table 9:** Comparison of experimental results with ANN model prediction for optimum conditions

| Response | Experimental result | Predicted value | Error  |
|----------|---------------------|-----------------|--------|
| MRR      | 315.36 mg/min       | 303.50 mg/min   | 3.76 % |
| EWR      | 1.65 mg/min         | 1.79 mg/min     | 8.49 % |
| SR       | 3.58 μm             | 3.73 μm         | 4.19 % |

The predicted optimum value of MRR is 303.50 mg/min, EWR is 1.79 mg/min and SR is 3.73 μm. Based on the experiments, the optimum value of MRR is 315.36 mg/min, EWR is 1.65 mg/min and of SR is 3.58 μm. The percentage error between experimental and predicted optimum values are 3.76 %, 8.49 % and 4.19 % for MRR, EWR and SR respectively.

**Conclusions**

This research work investigates the machining of 6061Al-SiC<sub>p</sub> by EDM using multi channel copper electrode by ANOVA and ANN prediction of various machining responses. Based on the results presented herein, the following can be concluded.

1. The electrical parameters more significantly affect the EDM machining process than the non-electrical parameter. The discharge current largely affects EWR whilst the pulse on time of EDM greatly affects either MRR or the SR.
2. The polarity of the workpiece also considerably affects the MRR or the EWR.
3. The ANN model developed is found to be suitable considering prediction accuracy and speed.
4. The average prediction error for MRR is 12.95%, EWR is 12.46 and in SR is 8.28%.
5. Satisfactory agreement between the experimental and proposed model results was obtained from using this type of network. Hence ANN can be used to successfully model EDM process, resulting in reliable predictions and providing a possible way to avoid time and money consuming experiments.
6. The percentage error between the optimum experimental and predicted results is in good agreement. Based on the significance of the output response required among MRR, EWR and SR, the suitable optimum condition can be selected.

### **Acknowledgments**

The authors are extremely thankful to Prof. P. G. Venkatakrishnan, M. E., Ph.D., Department of Metallurgical Engineering, Government College of Engineering, Salem, Tamilnadu, for the supply of the composite material and the management of JJ College of Engineering and Technology, Trichy, Tamilnadu for providing machining and measurements facilities.

### **Conflict of Interests**

The authors declare that they have no conflict of interest.

### **References**

- [1] Abeesh Basheer, C., Uday Dabade, A., Suhas Joshi, S., Bhanu Prasad, V.V., Gadre, V.M., Modeling of surface roughness in precision machining of metal matrix composites using ANN, *Journal of Materials Processing Technology* 197 (2008) 439-444.
- [2] Ho, K.H., Newman, S.T., State of the art electrical discharge machining (EDM), *International Journal of Machine Tools & Manufacture* 43 (2003) 1287-1300.
- [3] Krishna Mohana Rao,G., Rangajanardha,G., Hanumantha Rao, D., Sreenivasa Rao,M., Development of hybrid model and optimization of surface roughness in electrical discharge machining using artificial neural networks and genetic algorithm *Journal of Materials Processing Technology* 209 (2009) 1512-1520.



- [4] Mohan, B., Rajadurai, A., Satyanarayana, K.G., 2004. Electrical discharge machining of Al-SiC metal matrix composites using rotary tube electrode, *Journal of Materials Processing Technology* 153-154, 978-985.
- [5] Mohan Kumar Pradhan, Chandan Kumar Biswas, Neurofuzzy and neural network based prediction of various responses in electrical discharge machining of AISI D2 steel *International Journal of Advanced Manufacturing Technology* 50 (2010) 591-610.
- [6] Muthukrishnan, N., Paulo Davim, J., 2009. Optimization of machining parameters of Al/SiC-MMC with ANOVA and ANN Analysis, *Journal of Materials Processing Technology* 209, 225-232.

